

EXPERIMENTAL PERFORMANCE OF AN ADVANCED SOLAR-POWERED ADSORPTIVE ICE MAKER

Antonio Pralon Ferreira Leite

Departamento de Engenharia Mecânica, Universidade Federal de Campina Grande
Av. Aprígio Veloso, 882 - 58.109-970 Campina Grande-PB, Brasil antpralon@yahoo.com.br

Marcelo Bezerra Grilo

Departamento de Engenharia Mecânica, Universidade Federal de Campina Grande margrilo@hotmail.com

Francisco Antonio Belo

Laboratório de Energia Solar, Universidade Federal da Paraíba belo@les.ufpb.br

Rodrigo Ronelli Duarte de Andrade

Laboratório de Energia Solar, Universidade Federal da Paraíba rodrigo_ronelli@yahoo.com.br

Francis Meunier

Laboratoire du Froid, Conservatoire National des Arts et Métiers
292, Rue Saint Martin - 75141 Paris Cedex 03, France meunierf@cnam.fr

Abstract. This work presents an experimental analysis of the thermodynamic cycles in an adsorber of a solar-powered refrigerator prototype, applied to ice production, using the activated carbon-methanol pair. The adsorber consists of a series of tubes, placed side-by-side, making up the solar radiation absorber plate, whose surface was painted in matt black; the tubes back surface is also irradiated by use of two semi-cylindrical reflectors. The network of activated carbon-methanol isosters and the experimental cycles have been obtained from tests made over, under different meteorological conditions, specially concerning the cloud cover degree. Several data have been collected to evaluate the thermal efficiency of the adsorber-solar collector, and the refrigerator's performance, such as the temperatures in several points of the components, the total incident solar radiation, the ambient air temperature, the relative humidity and the wind velocity. The system was tested in a Brazilian region close to the Equator (7°8'S, 34°50'WG), during the October-December 2003 period. The cloud cover degree has demonstrated to be the main factor that limits the suitable system's functioning; even in days with high solar energy incidence, but cloudy sky, the adsorber did not allow an adequate condensation of methanol and, consequently, the frigorific effect was not sufficient to produce ice. For a typical clear sky day, the regenerating temperature reached 93.5°C, the condensed methanol mass was of 3 kg, and the machine produced 6 kg of ice per square meter at a temperature of -3,3°C, with a corresponding solar coefficient of performance (COP_s) of 0.085. These results have been compared with those from a prototype tested in Tunisia (35°45'N, 10°45'WG), using a flat adsorber with selective surface and a single glass cover, and the same adsorptive pair.

Keywords: Adsorption, Activated Carbon-Methanol, Solar Refrigeration

1. Introduction

Solar refrigeration is one of the attractive applications of solar energy because both the insulation supply and the demand for cooling are largest in the same period. The solar ice production could be important in developing countries for storage of agricultural products, food and medicines, especially in remote non-electrified areas. In the last two decades, different solar technologies have been proposed and tested, for the main component of autonomous sorption cooling systems, in order to become them economically viable. All of these systems are based on one of the following technological choices: liquid absorption, solid absorption (chemical reaction), or adsorption. As compared to the other above-mentioned techniques, adsorption presents some important advantages: during the sorption processes, the adsorbent does not need a rectifying column as in the liquid absorption, and it is not submitted to any change in volume as in solid absorption. Moreover, adsorption techniques allow the cycling of large amounts of refrigerant fluid. On the other hand, their main disadvantages are the low coefficients of performance and the need of long periods for the adsorption completion.

In relation to the solar adsorptive refrigeration systems, different types of solid-gas pairs have been considered. The zeolite-water (Chaya et al., 2003; Grenier et al., 1988) and silica gel-water (Buchter et al., 2001; Tangkengsirisin et al., 1998) were chosen for cold storage, while the activated carbon-methanol pair was chosen for ice production (Boubakri et al., 1992; Lemini et al., 1992). The activated carbon-ammoniac pair (Tamainot-Telto and Critoph, 1997) was also employed for low temperatures refrigeration applications using solar energy.

Solar ice making by adsorption could be appropriate, however it needs both good heat conversion and heat release from the adsorber. The development of adsorptive systems is still limited by the adsorber-solar collector component cost, and by the intermittence of the incident solar radiation, which makes it difficult to be competitive with

conventional compression systems. Different technologies for solar adsorptive devices have been tested to increase the ice production and to reduce its manufacturing cost, as shown in a recent study (Boubakri, 2003).

This paper concerns a multi-tubular adsorber, as component of a solar-powered system based on adsorption processes, applied to ice production, which is one basic need in developing countries, primarily for food and vaccine conservation. The actual adsorptive icemaker prototype utilizes a soft technology for the thermal solar conversion, appropriate for a daily intermittent cycle. The collector is technically simple; it is static and bi-facially irradiated, in conjunction with a transparent insulation cover highly efficient. Other technical innovations were considered, in relation to most of the units already constructed and tested, especially in France, where the adsorber always had the shape of a box with extended surfaces, and air condensers have been widely used. All components of the present machine are multi-tubular and it uses a water condenser.

In order to improve the collector's performance the adsorber-solar was covered by two transparent plates filled out with a polycarbonate honeycomb element, known as *transparent insulation material* (Rommel and Wagner, 1992; Buchberg and Edwards, 1976), or TIM cover. Reflectors were installed down below the tubes to allow the solar incidence to reach also the lower face of the adsorber. Activated-carbon is used as adsorbent and it is placed inside the tubes whose surface is the solar radiation absorber plate; methanol is used as adsorbate, or working fluid.

2. Adsorption refrigeration thermodynamic cycle

The adsorption icemaker is based on an intermittent cycle, which occurs without heat recovering. This cycle consists of two typical stages: one is characterized by the adsorption process, when the evaporation of the working fluid (the adsorbate) takes place; and another consists of the solid medium (the adsorbent) regeneration by solar energy, when the adsorbate is condensed. The solar-powered refrigerator is mainly composed of an integrated adsorber-solar collector, connected to a condenser and an evaporator (Fig. 1). The direction of the gaseous flow is altered, according to the cycle stage; it goes from the adsorber towards the condenser during the regeneration, and from the evaporator towards the adsorber, during the adsorption phase. During the refrigeration stage, the TIM covers are removed to improve the heat dissipation from the adsorber, as shown in Figures 1 and 9.

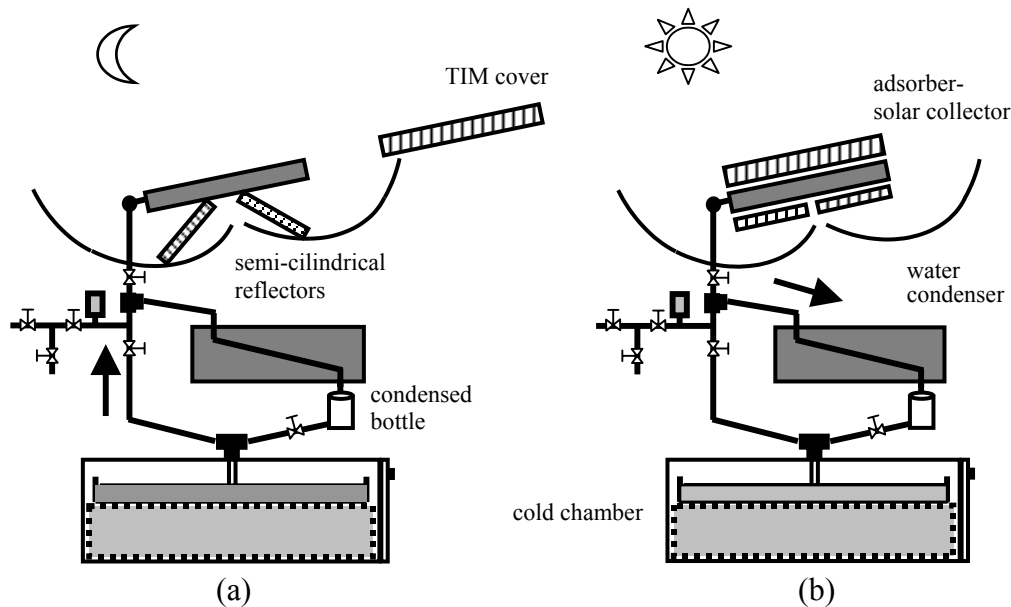


Fig. 1. Scheme of the adsorptive icemaker and its operation: (a) Stage of refrigeration; (b) Stage of regeneration.

The refrigeration stage begins by the end of the afternoon, when the temperature and the pressure of the adsorber decrease, following an isosteric process, i.e., a process in which the adsorbed phase concentration (a) is constant. The evaporation takes place when the gaseous adsorbate flows to the adsorber throughout the night, producing the refrigeration effect until the adsorber temperature reaches a minimum value. In another isosteric process, the adsorber is heated by the solar radiation incidence, increasing the temperature and pressure until they reach the condenser pressure. Then condensation takes place and the adsorbate is transferred to the condenser until the adsorber reaches a maximum temperature, which means the end of the cycle. The ideal thermodynamic cycle can be represented by two isosters (iso-lines with constant adsorbed phase concentration) and two intercalated isobars, as shown in Fig. 2. Processes 1-2 and 2-3 represent the cooling of the adsorbent and the adsorption, respectively, and processes 3-4 and 4-1 describe the

regeneration stage of the adsorbent (heating and desorption). A complete thermodynamic analysis of the adsorption refrigeration system is given by Leite (1998).

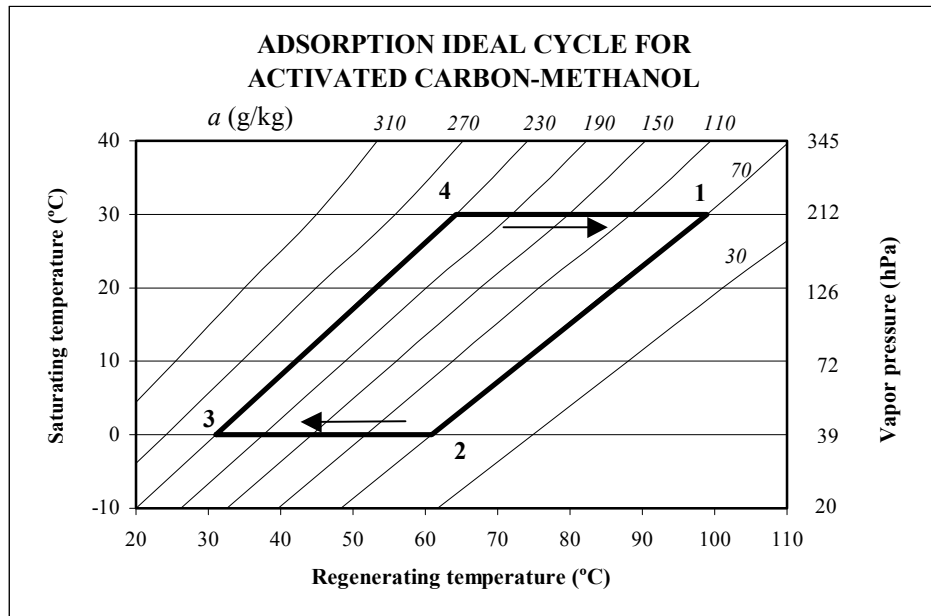


Fig. 2. Network of activated carbon-methanol isotherms and theoretical cycle.

3. Description of the solar-powered adsorptive icemaker

The present prototype has been designed and built after results from numerical simulations utilizing meteorological data of João Pessoa (7°8'S, 34°50'WG), northeast of Brazil, whose climate is typically hot and humid, as presented by Leite and Dagueuet (2000). These calculations were based on a projected collector area of 1 m², and the radiative properties of the absorber surface were those for a selective coating. A general view of the actual prototype with their components is shown in Fig. 3. The main components are a multi-tubular adsorber (Fig. 4) integrated to a bifacially irradiated solar collector (Fig. 5), a water condenser, an evaporator and a cold chamber. All these components are multi-tubular and made from stainless steel.



Fig. 3. General view of the prototype.



Fig. 4. Multi-tubular adsorber.

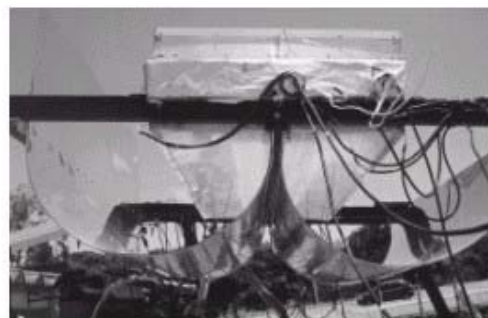


Fig. 5. Integrated adsorber-solar collector.

The adsorber is composed by 8 tubes placed side-by-side (Fig. 4), covering a 0,61 x 1,65 m² area, and the adsorbent occupies an annular space between the front of the collector surface and the axial tube formed by a metal net,

through which the refrigerant fluid diffuses (Fig. 6). The quantities of activated carbon and methanol introduced in the system are 21 kg and 6 kg, respectively. The surface of the tubes constitutes the solar absorbing surface, and it is painted in matt black. To allow an incidence of solar radiation on both its faces semi-cylindrical reflectors are installed below the adsorber, as shown in Fig. 5.

The TIM covers installed in the adsorber are schematically shown in Fig. 7. The collector bottom is also insulated by a TIM cover (Fig. 8) to allow a bifacial irradiation of the adsorber, by means of aluminium polished reflectors positioned below the tubes plan (Fig. 5), as proposed by Goetzberger et al. (1992). The honeycomb structure cells have an average diameter of 3 mm, and TIM heights are respectively 80 mm for the upper cover, and 60 mm for the lower cover, and they are delimited by a plate of glass and another of compact polycarbonate, this last placed close to the adsorber, having thickness of 4 mm and of 3 mm, respectively for the upper and lower covers. Air gaps were left between the adsorber and the polycarbonate plate: 25 mm for the upper cover and 15 mm for the lower cover.

The lower TIM cover was made in two identical parts (Figs. 8 and 9), articulated around a central and longitudinal axis, in order to be movable (Fig. 9), which improves the heat dissipation from the adsorber, during the refrigeration stage. According to Boubakri et al. (2003) and Buchter et al. (2003), with an efficient nocturnal cooling of the adsorber-collector, the performance of the machine should increase about 35%.

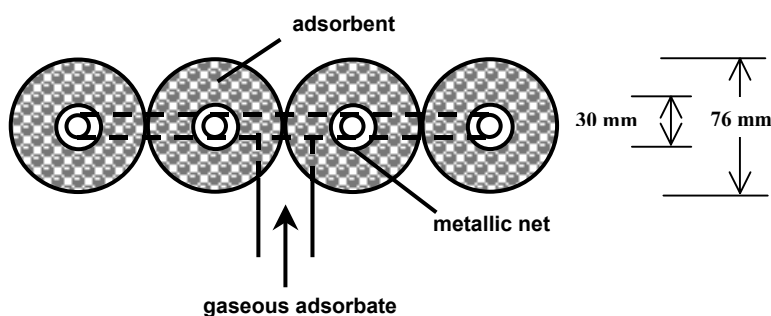


Fig. 6. Schemematic view of the multi-tubular adsorber.

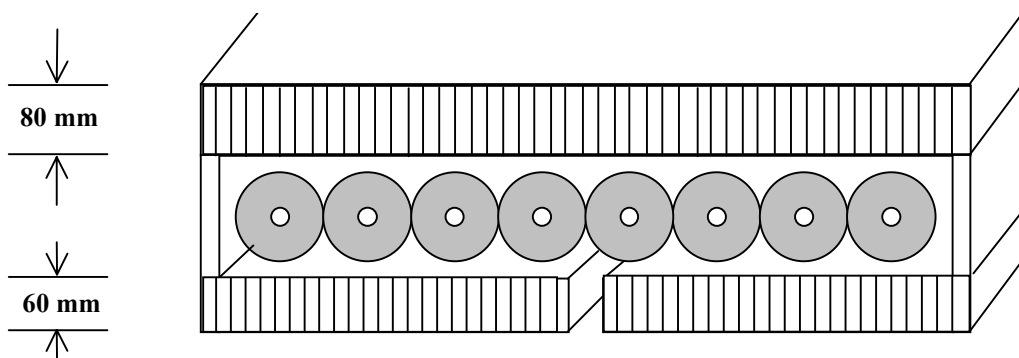


Fig. 7. Schematic view of the TIM covers over and under the adsorber.

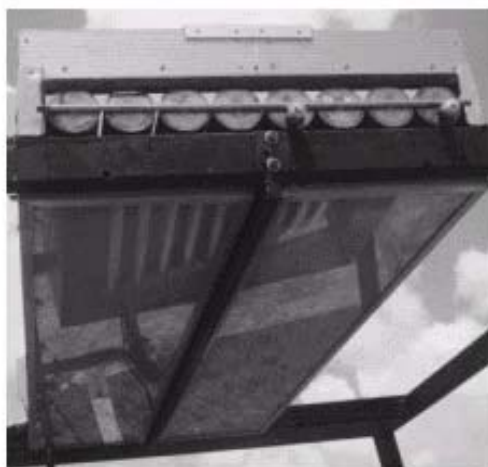


Fig. 8. TIM covers positioned during the regeneration stage.



Fig. 9. TIM covers positioned during the refrigeration stage.

4. Experimental procedure

4.1 Parameters measurement

Temperatures measured, in different points of each component of the prototype, using termoresistive sensors Pt-100, were recorded at each hour during a whole day. To evaluate the longitudinal temperature distribution on the absorbing surface, eight sensors were positioned on a central tube. For the transversal distribution, four sensors were installed at the middle plan, and to obtain an average value for the upper face of the adsorber, temperatures have been measured in four points at each extremity, both over and bellow the tubes. Besides, the pressure has been measured with a piezometric sensor installed between the adsorber and the condenser.

The adsorbed phase concentration was determined by a direct measurement of the volume of condensed methanol, through a transparent graduated reservoir installed between the condenser and the evaporator (Figs. 1 and 3). The temperatures have also been measured at other points of the system, such as in the water and on the tubes of the condenser, in the water to be frozen, on the tubes of the evaporator, on the roof of the cold chamber, on the external faces of both upper and lower TIM cover, and on the reflectors. The following meteorological parameters have also been measured: total solar radiation, ambient air temperature, relative humidity, and wind velocity. To evaluate the cloud cover degree, especially during the night, empirical observations were made; the sky was classified, according to the predominant conditions, in three categories: cloudless (clear sky), partly cloudy and completely cloudy.

4.2 Adsorbate flow directing

Since the cycle is intermittent, and to guarantee the condensed adsorbate measurement, two valves have been used to direct the adsorbate flow according to the stage (Fig. 10). For the adsorption stage, when the working fluid flows towards the adsorber, one valve (V1) positioned between the adsorber and the evaporator is opened, while another one (V2) installed between the condenser and the evaporator, is closed. For the regeneration stage, V1 is closed, forcing the methanol to flow towards the condenser, while V2 remains closed, to allow for the measurement of the condensed volume in the graduated bottle. Immediately before the adsorption process begins, V2 is open, the liquid methanol is transferred to the evaporator, and then, when V1 is opened, the evaporated adsorbate moves towards the adsorber.

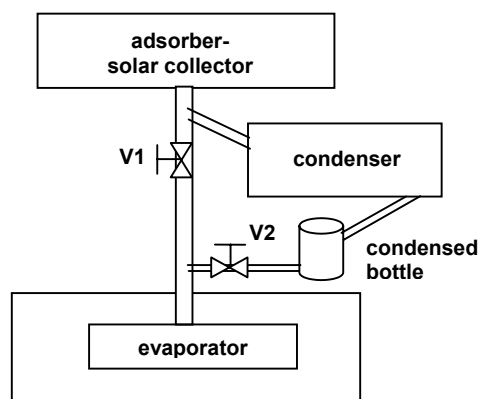


Fig. 10. Scheme of the valves position for directing the adsorbate flow.

For a regular functioning of the machine, the above-mentioned procedure is not necessary, because the refrigerating product, i.e., ice, is removed from the cold chamber at the end of each daily cycle. Therefore, there is no problem if some amount of adsorbate is condensed directly in the evaporator, in the beginning of the regeneration stage. On the other hand, this situation could be even considerate adequate, since it helps in the ice removing through the latent heat of the changing phase over the tubes of the evaporator.

5. Results and discussion

Several tests were performed along October-December 2003. Table 1 shows the atmospheric and operational conditions, as well as some physical parameters, for the cycles obtained for 10.5-6.2003 (cycle 1), 11.29-30.2003 (cycle 2) and 12.8-9.2003 (cycle 3). Each one represents a specified cloudy night sky condition, as above described.

Tables 2 to 4 show the values of the absorber plate temperature (T_p), the adsorbent temperature (T_{ac}), pressure (P) and concentration (a), for the limit points concerning cycles 1, 2 and 3, respectively. The cycles have always been initiated immediately after the repositioning of the TIM covers, over and under the adsorber, at 4:00 a.m. Adsorption

has always begun at 7:00 p.m., at the same moment the valve installed between the evaporator and the adsorber was opened. The maximum regeneration temperatures have been registered around 1:00 p.m., for the three cycles.

Table 1. Atmospheric and operational conditions, and physical parameters for each cycle.

CYCLE	Cycle 1 (10/5-6)	Cycle 2 (11/29-30)	Cycle 3 (12/8-9)
Predominant conditions of night sky	clear	partially cloudy	totally cloudy
Opening time of lower TIM cover	14:00	13:30	13:40
Opening time of upper TIM cover	19:00	13:30	13:40
Hourly incident solar energy (MJ m ⁻²)	23,7	23,2	23,3
Condensed methanol mass (kg)	3,0	2,0	2,3
Adsorber-solar collector (β)	3,3°N	9,5°S	9,5°S
Incidence angle at solar noon (θ_{sn})	2,0°	5,2°	6,3°

Table 2. Values of the ambient temperature (T_{amb}) and the adsorber's properties (T_p , T_{ac} , P e a) at the limit points for cycle 1 (10/5-6/2003).

LIMIT POINTS	Local Time	T_{amb} (°C)	T_p (°C)	T_{ac} (°C)	P (h Pa)	a (kg kg⁻¹)
Regeneration's start	4:00	25.6	24.3	25.8	26	0.220
Desorption's start	9:25	30.5	74.6	71.7	192	0.176
Maximum temperature	13:00	31.0	100.1	93.5	221	0.087
End of desorption	13:57	30.6	60.7	84.0	127	0.077
Adsorption's start	19:00	26.2	33.3	49.2	27	0.090
End of adsorption	3:20	24.7	23.7	24.3	26	0.230

Table 3. Values of the ambient temperature (T_{amb}) and the adsorber's properties (T_p , T_{ac} , P e a) at the limit points for cycle 2 (11/29-30/2003).

LIMIT POINTS	Local time	T_{amb} (°C)	T_p (°C)	T_{ac} (°C)	P (h Pa)	a (kg kg⁻¹)
Regeneration's start	4:00	25.7	26.2	25.6	31	0.240
Desorption's start	9:37	29.7	66.5	64.7	204	0.220
Maximum temperature	13:00	29.9	87.3	82.6	236	0.147
End of desorption	13:25	31.3	84.0	82.3	234	0.145
Adsorption's start	19:00	26.4	27.1	39.6	38	0.150
End of adsorption	2:00	25.8	25.0	24.6	28	0.245

Table 4. Values of the ambient temperature (T_{amb}) and the adsorber's properties (T_p , T_{ac} , P e a) at the limit points for cycle 3 (12/8-9/2003).

LIMIT POINTS	Local time	T_{amb} (°C)	T_p (°C)	T_{ac} (°C)	P (h Pa)	a (kg kg ⁻¹)
Regeneration's start	4:00	26.6	26.2	26.6	32	0.237
Desorption's start	9:37	31.6	65.3	64.5	210	0.230
Maximum temperature	13:00	31.5	92.7	86.7	242	0.128
End of desorption	13:25	31.9	89.5	86.9	244	0.127
Adsorption's start	19:00	26.7	29.1	42.1	41	0.175
End of adsorption	2:00	24.7	24.0	24.1	30	0.235

The thermodynamic cycles obtained experimentally are given in a pressure-temperature diagram, as shown in Figures 11 to 13. For each one of the cycles, the hours for each respective limit points are indicated. The differences between two consecutive hour cycles determine the duration of each one of the four basic processes that constitutes the cycle.

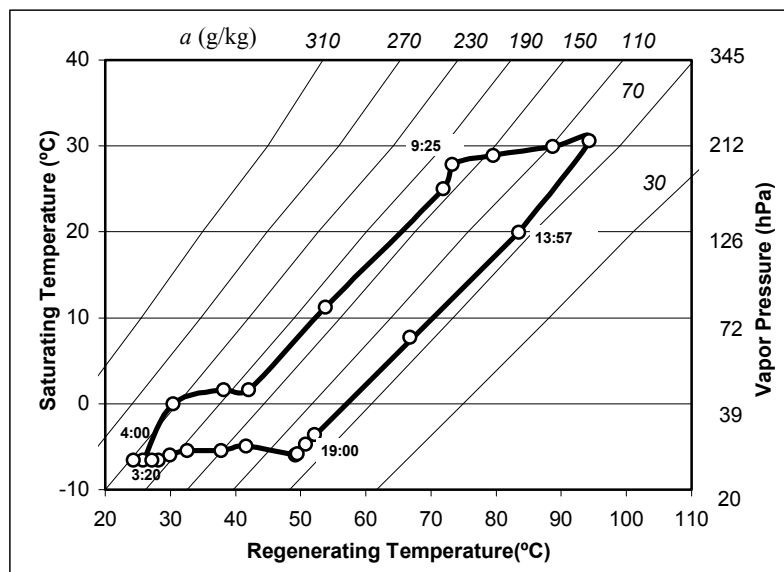


Fig. 11. Experimental adsorption refrigeration cycle for October 5-6, 2003 (cloudless).

Analyzing the cycles easily allows us to obtain the extreme temperatures concerning the desorption and the adsorption processes, as given in Tables 2 to 4. Moreover, another practical aspect of the adsorption cycles consists in obtaining directly the minimum temperature of the saturated methanol inside the evaporator. For the analyzed cycles 1, 2 and 3, the values were about -6.5°C, -5.5°C and -5.0°C, respectively.

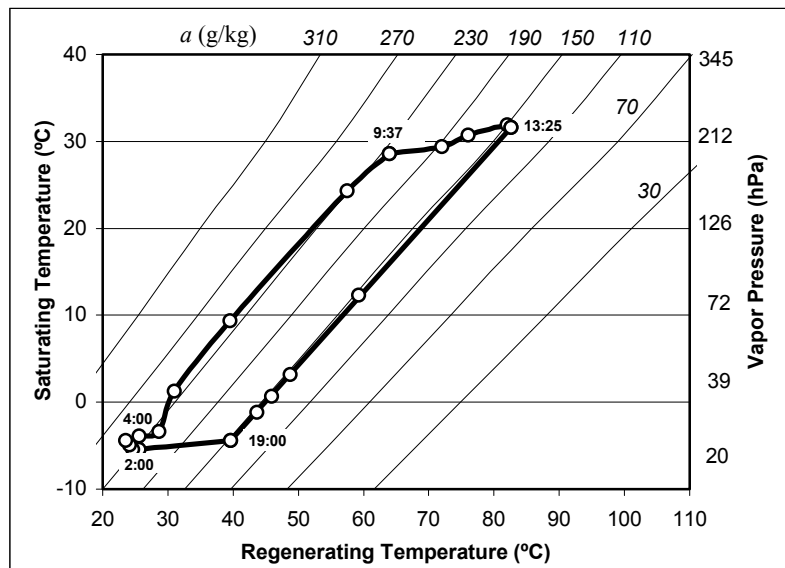


Fig. 12. Experimental adsorption refrigeration cycle for November 29-30, 2003 (partly cloudy).

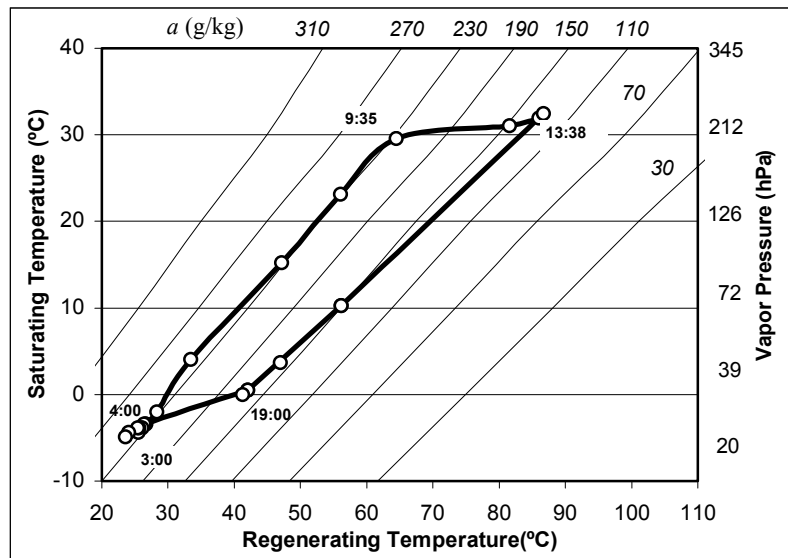


Fig. 13. Experimental adsorption refrigeration cycle for December 8-9, 2003 (cloudy).

5.1 Duration of the desorption process

According to the limit point hours indicated in the cycles, the larger duration of the desorption period (4 h 32') occurred in cycle 1. Thus, the larger concentration variation that has been verified during this cycle could be experimentally proved, through the direct measurement of the condensed methanol in a transparent bottle. This can be explained by the incident solar energy on October 5th, for cycle 1, which was more intense than during the other cycles, due to the very low cloud cover degree verified, which made possible an important predominance of beam radiation, especially during the 10:00 a.m. to 1:00 p.m. period. This means that the adsorber could utilize more efficiently the incident solar energy. In fact, the components of the adsorber-solar collector, as TIM covers and reflectors, are more appropriate to receive and transmit the beam radiation to the absorber plate than diffuse radiation. For the other cycles, although the daily solar radiation has been similar for both, when the radiation data are compared, we observe that the beam component for December 8th was larger than for November 29th, especially in the 10:00 a.m. till noon period. Consequently, for cycle 3, the regeneration temperatures were larger than those obtained for cycle 2, as well as the amount of condensed methanol, as given in Tables 1 and 5.

5.2 Duration of the adsorption process

From the comparative analysis of the adsorption process for the three cycles, we verify that the concentration increase occurs much more slowly in cycle 1 than in the other cycles. This can be clearly observed in cycles 2 and 3 by the agglomerate of points measured close to the larger isoster, while in cycle 1 these points are somewhat scattered during the adsorption. According to the recorded times at the limit points (Figs. 10, 11 and 12), the larger adsorption period has been verified in cycle 1, totalizing 8 h and 20'. This could be explained by three factors: larger amount of previously condensed methanol, TIM covers opening later (at 7:00 p.m.), and predominant night sky conditions. In this cycle, the sky has remained basically clear, throughout the adsorption process. This improves the radiative exchanges and, consequently, causes a decrease in the adsorption temperature that makes possible a more intensive gaseous methanol transfer to the adsorber. For cycle 3, adsorption has been relatively long (8 h), because some light rain occurred in the last hour of the process, reducing the adsorber temperature even more.

Table 5 shows the main parameters obtained for desorption and adsorption processes for the three cycles. These values show that only for cycle 3 the quantity of evaporated methanol was smaller than that of condensed. In fact, in this cycle only more than half of the condensed mass (55%) was used to produce the cooling effect. The final results about the ice production obtained in each cycle have demonstrated that the evaporation of this quantity of methanol (1.3 kg) was not enough to freeze the water, as shown in Table 6.

Table 5. Duration of the desorption and adsorption, concentration variations and masses of condensed and evaporated methanol for the obtained cycles.

CYCLE	Cycle 1 (10/5-6)	Cycle 2 (11/29-30)	Cycle 3 (12/8-9)
Desorption's duration	4 h 32'	3 h 48'	4 h 03'
Δa in regeneration (g kg^{-1})	143	95	110
Mass of condensed methanol (kg)	3,0	2,0	2,3
Adsorption's duration	8 h 20'	7 h 00'	8 h 00'
Δa in adsorption (g kg^{-1})	141	95	60
Mass of evaporated methanol (kg)	3,0	2,0	1,3

5.3 Deviation of the actual cycle from the ideal cycle

The resulting thermodynamic cycles differ from the theoretical cycles, mainly in relation to the desorption and adsorption processes, because they were not isobaric, as in the ideal cycle shown in Figure 2. As for the desorption, this happened because, during the methanol transfer to the condenser, the adsorber has suffered a large temperature variation, due to the solar radiation incidence, and the efficient conversion of this energy in heat. During this process, the adsorbent temperature is much more influenced by the atmospheric conditions than during the adsorption. The adsorption is more similar to an isobar, because the temperature variations in the adsorber during the night are smaller, influenced basically by the ambient air conditions (temperature and velocity) and by the cloud cover degree around the zenith. In cycle 1, because the night sky has remained predominantly clear, it has been possible to obtain a long evaporation period, and, then, saturating temperatures low enough to produce an appropriate amount of ice. In cycles 2 and 3, the evaporation happened very quickly, not allowing an isobaric process. Although in cycle 3 the adsorbent temperature has been lower at the end of the adsorption, comparatively to cycles 1 and 2, the cloudy sky did not make it possible to obtain temperatures and pressures low enough to produce ice.

In relation to the isosteric processes, small deviations are observed, in the adsorber heating and cooling, for all cycles. For cycles 1 and 2, the concentration has remained practically constant in both processes, but, for cycle 3, some readsorption was noticed before the opening of the valve between the adsorber and the evaporator. By the way, this valve has always been opened at the same hour (7:00 p.m.) for the three cycles. The total amount of condensed methanol has been considered equivalent to the concentration variation in the adsorbent, at the end of the regeneration process. The instabilities recorded in the beginning of the regeneration processes, particularly stressed in cycle 1, are a consequence of opening the cold chamber to remove the ice and inject new water, with the subsequent repositioning of the TIM covers.

The instabilities recorded in the beginning of the regeneration processes, particularly stressed in cycle 1, are a consequence of opening the cold chamber to remove the ice and inject new water, with the subsequent repositioning of the TIM covers.

5.4 Refrigeration system properties

The parameters of the components inside the cold chamber at the end of each cycle, such as the saturating temperature (T_{sat}), evaporator temperature (T_{evap}), water to be frozen (T_{water}), condensed methanol mass (M_{cond}), and the ice mass produced (M_{ice}), are presented in Table 6. These values show that, although in cycle 3 the amount of condensed methanol has been 15% larger than that verified for cycle 2, the minimum adsorption temperatures for this cycle have been smaller than those obtained for cycle 3. This can be explained by the night sky conditions for each one of the cycles; during cycle 3 the sky has been predominantly cloudy, while during cycle 2 it stayed only partially cloudy. During cycle 1, the night sky has been ideal, i.e., basically cloudless, allowing for temperatures low enough in the adsorber to ensure adsorption and, consequently, promoting a larger cooling effect.

Table 6. Minimum temperatures inside the cold chamber, and mass of ice produced for each cycle.

CYCLE	T_{sat} (°C)	T_{evap} (°C)	T_{water} (°C)	M_{cond} (kg)	M_{ice} (kg)
Cycle 1 (10/5-6/03)	- 6.6	- 4.6	- 3.3	3.0	6.05
Cycle 2 (11/29-30/03)	- 5.5	- 2.5	- 1.5	2.0	2.10
Cycle 3 (12/8-9/03)	- 4.9	- 1.8	- 0.5	2.3	0

The system's performance has demonstrated a high sensitivity to the night sky conditions, even under a good solar irradiation in the previous regeneration stage. It has been shown that the long wave infrared radiation exchanged between the adsorber and the sky is the most important limiting factor for a suitable operation of the system. By the way, even under clear sky conditions the experiments have demonstrated the need to remove also the upper TIM cover, after the regeneration stage. It has been verified that for cloudy night skies, the temperature of the water inside the cold chamber can decrease below 0°C, but at insufficient levels for freezing, as shown in Table 6. Only for clear skies, especially around the zenith, the temperature on the evaporator has reached appropriate values to freeze the water.

Table 7 shows the limit values, obtained for clear sky (cycle 1), of the regeneration temperature ($T_{reg(max)}$), adsorption temperature ($T_{ads(min)}$), and evaporation temperature ($T_{eva(min)}$), the mean condensation temperature ($T_{con(mean)}$), masses of condensed methanol (M_{con}) and of ice produced (M_{ice}), daily solar energy irradiation (E_i). These values are compared with those obtained from a prototype tested in Monastir (35°45'N, 10°45'WG), Tunisia (Medini et al., 1991), using the same adsorptive pair, a water condenser, a flat adsorber-solar collector with selective surface and a single glazing cover.

Table 7. Experimental system parameters and solar thermal efficiency for cycle 1 (October 5-6, 2003).

System	$T_{reg(max)}$ °C	$T_{ads(min)}$ °C	$T_{con(mean)}$ °C	$T_{eva(min)}$ °C	E_i MJm ⁻²	M_{cond} kg	M_{ice} Kgm ⁻²
Present prototype	93.5	24.3	30.0	- 4.6	23.7	3.0	6.05
Tunisian prototype ¹	90.0	12.0	27.5	- 2.0	25.0	2.5	5.00

1. In reference (Medini et al., 1991).

The difference between the mean daily solar thermal efficiencies (η) for the Tunisian prototype (41%) and for the present prototype (65%) proves the excellent performance of the TIM covers. According to Leite et al. (2003), the average values of the experimental overall heat loss coefficient at the top (U_t) and at the bottom (U_b) of the present adsorber-solar collector were 1.34 Wm⁻²K and 1.18 Wm⁻²K, respectively, while for the selective surface adsorber with single glazing cover U_t was about 5 Wm⁻²K. In spite of the very high solar thermal efficiency verified, the quantity of ice produced with the present machine was only 21% higher than that obtained by the Tunisian icemaker.

For the present system, the solar coefficient of performance (COP_s), defined as the ratio of the effective cooling load to the incident solar energy (E_i) that passes directly through the collection plan of the adsorber, was of 0.085, which is about 27% larger than that obtained for the Tunisian prototype ($COP_s = 0.067$). This can be explained by the significant differences in the ambient air temperatures, as shown in Table 6; the lower temperature at Monastir facilitates the adsorption process and, hence, the refrigeration effect. Boubakri et al. (2000) have carried out a long term experimental study with methanol-carbon adsorptive solar icemakers, in which the adsorber-collector is integrated to an air condenser, the called collector-condenser technology. They have obtained the following yearly average results: diurnal and nocturnal ambient temperatures of 24°C and 15°C, a daily ice production around 4 kgm⁻², for an incident total solar radiation of 19.5 MJm⁻², with a corresponding net solar coefficient of performance of 0.069. Although this COP_s value is about 19% smaller, for the present prototype the daily ice production was 50% larger, certainly because with the proposed solar technology (bifacially irradiated collector + TIM covers) the regenerating energy is more efficiently used, allowing to condense a larger amount of methanol.

6. Conclusion

The multi-tubular adsorber of a solar-powered adsorptive icemaker using a bi-facially irradiated collector has been experimentally evaluated. Its solar thermal efficiency has been compared to a similar machine using selective surface and a single glazing cover, tested in Tunisia. The present system's efficiency was shown to be significantly better, due to the use of devices to decrease the heat losses from the adsorber to the ambient air. The mean thermal efficiency of the present adsorber-solar collector was about 58% higher than that obtained for the flat adsorber used in the Tunisian prototype. The use of reflectors improves both the solar incidence and the heat dissipation of the adsorber during the refrigeration stage, by increasing the radiative exchanges with the sky. The cloud cover degree has demonstrated to be the main factor that limits the suitable system's functioning; even in days with high solar energy incidence, but cloudy sky, the adsorber did not allow an adequate condensation of methanol and, consequently, the frigorific effect was not sufficient to produce ice. For a clear sky day, the regeneration temperature reached 93.5°C, the condensed methanol mass was of 3 kg, and the machine produced 6 kg of ice per square meter at a temperature of -3,3°C.

7. Acknowledgements

The authors gratefully acknowledge the Brazilian agency, National Council of Scientific and Technological Development - CNPq, for the financial support provided to this work through Research Project Grant No. 522637/96-5.

8. References

- Boubakri, A., 2003, "A new conception of an adsorptive solar-powered ice maker", *Renewable Energy*, Vol. 28, pp. 249-263.
- Boubakri, A., Arsalane, M., Yous, B., AliMoussa, L., Pons, M. and Meunier, F., 1992, "Experimental study of adsorptive solar powered ice-makers", *Renewable Energy* Vol. 2, pp. 7-15.
- Boubakri, A., Guilleminot, J. J. and Meunier, F., 2000, "Adsorptive solar powered ice maker: Experiments and model", *Solar Energy*, Vol. 69, pp. 249-263.
- Bougard, J. and Veronikis, G., 1992, "Adsorbent modulaire pour machine frigorifique solaire charbon actif-ammoniac. Proceedings of the Meeting on Solid Sorption Refrigeration, Paris, France, Vol. 1, pp. 302-307.
- Buchberg, H. and Edwards, D. K., 1976, "Design considerations for solar collectors with cylindrical glass honeycombs", *Solar Energy*, Vol. 18, pp. 193-203.
- Buchter, F., Hildebrand, C., Dind, Ph. and Pons, M., 2001, "Experimental data on an advanced solar-powered adsorption refrigerator", *Proceedings of the Heat Powered Cycles Conference (HPC'01)*, Paris, France.
- Buchter, F., Dind, Ph. and Pons, M., 2003, "An experimental solar-powered adsorptive refrigerator tested in Burkina-Faso", *Int. Journal of Refrigeration*, Vol. 26, pp. 79-86.
- Chaya, M. R., Horn, M., Spinoza, R. and Leite A. P. F., 2003, "Evaluation of a zeolite-water solar adsorption refrigerator". *Proceedings of the Solar World Congress (ISES'2003)*, Göteborg, Sweden.
- Goetzberger, A., Dengler, J., Rommel, M., Göttische, J. and Wittwer, V. A., 1992, "A new transparently insulated, bifacially irradiated solar flat plate collector", *Solar Energy*, Vol. 49, No. 5, pp. 403-411.
- Grenier, Ph., Guilleminot, J.J., Meunier, F., Pons, M., 1988, "Solar powered solid adsorption cold store. *J. Solar Energy Engng.*, Vol. 110, pp. 192-197.
- Leite, A. P. F., 1998, "Thermodynamic analysis and modelling of an adsorption-cycle system for refrigeration from low-grade energy sources", *Journal of the Brazilian Society of Mechanical Sciences*, Vol. 20 (3), pp. 301-324.
- Leite, A. P. F. and Daguene, M., 2000, "Performance of a new solid adsorption ice maker with solar energy regeneration", *Energy Conversion & Management*, Vol. 41, pp. 1625-1647.

- Leite, A. P. F., Belo, F. A., Grilo, M. B. and Andrade, R. R. D., 2003, "Experimental evaluation of a multi-tubular adsorber covered with transparent insulation material", Proceedings of the 6th Mechanical Engineering Iberian-American Congress (CIBEM6), Coimbra, Portugal.
- Lemini, F., Buret-Bahraoui, J., Pons, M. and Meunier, F., 1992, "Simulation des performances d'un réfrigérateur solaire à adsorption: 1. Comparaison des performances pour deux types de charbon actif", *Revue Int. du Froid*, Vol. 5, pp. 159-167.
- Medini, N., Marmottant, B., Golli, E. S. and Grenier, Ph., 1991, "Etude d'une machine solaire à fabriquer de la glace", *Revue Int. du Froid*, Vol. 14, pp. 363-367.
- Rommel, M. and Wagner, A., 1992, "Application of transparent insulation materials in improved flat-plate collectors and integrated collector storages", *Solar Energy*, Vol. 49, No. 5, pp. 371-380.
- Tamainot-Telto, Z., Critoph, R. E., 1997, "Adsorption refrigerator using monolithic carbon-ammonia pair", *Int. Journal of Refrigeration* Vol. 20, No. 2, pp. 146-155.
- Tangkingsirisin, V., Kanzawa, A. and Watanabe, T., 1998, "A solar-powered adsorption cooling system using a silica gel-water mixture", *Energy* Vol. 5, pp. 347-353.